HHS Public Access
Author manuscript
FASEB J. Author manuscript; available in PMC 2024 August 01.

Published in final edited form as:
FASEB J. 2023 August ; 37(8): e23106. doi:10.1096/fj.202200705RR.

Disrupted glucose homeostasis and glucagon and insulin secretion defects in Robo βKO mice

Melissa T. Adams[1,*], **Bayley J. Waters**[1,*], **Sutichot D. Nimkulrat**[1], **Barak Blum**[1,†]

[1]Department of Cell and Regenerative Biology, University of Wisconsin-Madison, Madison, WI 53705, USA

Abstract

The axon guidance proteins, Roundabout (Robo) receptors play a critical role in morphogenesis of the islets of Langerhans. Mice with a β cell-selective deletion of Robo (Robo βKO), show severely disrupted spatial architecture of their islets, without defects in β cell differentiation or maturity. We have recently shown that Robo βKO mice have reduced synchronous glucose-stimulated β cell calcium oscillations in their islets *in vivo*, likely disrupting their pulsatile insulin secretion. Here, we analyze whole-body metabolic regulation in Robo βKO mice. We show that Robo βKO mice have mild defects in glucose homeostasis, and altered glucagon and insulin secretion. However, we did not observe any severe whole body glucoregulatory phenotype following the disruption of islet architecture in Robo βKO. Our data suggest that islet architecture plays only a mild role in overall glucoregulation.

Graphical Abstract

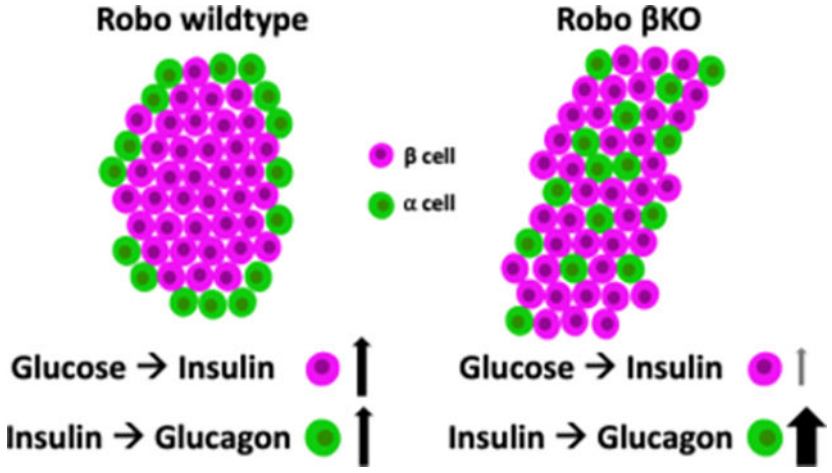

†**Corresponding Author:** Barak Blum; bblum4@wisc.edu.
*Equally contributing authors

Author Contributions

Conceptualization, B.B. and M.T.A.; Methodology, B.B. and M.T.A.; Investigation, M.T.A., B.J.W., and S.D.N.; Formal Analysis, M.T.A., B.J.W., and S.D.N.; Writing— Original Draft, B.B. and M.T.A.; Writing, Review, and Editing, all authors; Funding Acquisition, B.B.; Supervision, B.B.

Conflict of Interest Statement

All Authors have stated explicitly that there is no conflict of interest in connection to this article.

In Robo βKO mice, disrupted islet architecture leads to loosening of fine intra-islet regulation, resulting in lower secretion of insulin from β cells and higher secretion of glucagon from α cells in the disorganized islet.

Introduction

The islets of Langerhans control glucose homeostasis through coordinated hormone secretion. There are at least five different types of islet endocrine cells, which are characterized by the hormones they produce. The three most common are the insulin-producing β cell, the glucagon-producing α cell, and the somatostatin-producing δ cell. Within the rodent islet, endocrine cells are organized such that β cells preferentially reside in the core, while non-β endocrine cells reside in the periphery[1]. In humans, islet architecture is more complex[2,3], but is still non-random and governed by the preferential formation of homotypic interactions between endocrine cells[4–6].

The number and type of homotypic and heterotypic cell-cell interactions within the islet are important for intra-islet paracrine signaling and the electrical cell-cell coupling required to coordinate the interdependent pulsatile patterns of insulin, somatostatin, and glucagon secretion[7,8]. In response to elevated glucose, β cells co-secrete insulin in a synchronized, pulsatile pattern allowed for by the high level of gap-junctional coupling among intra-islet β cells, a property made possible by the preferential tendency for homotypic β-β contacts within the islet[9–12]. Pulsatile insulin secretion, coordinated systemically amongst all islets in the pancreas, is important for preserving insulin sensitivity of peripheral tissues, and for robust activation of hepatic insulin signaling[13–15]. Pulsatile β cell secretion within the islet during elevated glucose also stimulates pulsatile glucagon and somatostatin secretion from neighboring α and δ cells, respectively, *via* paracrine signaling. In addition to intra-islet paracrine signaling, juxtacrine signaling such as EphA and ephrinA occurs between homotypic β-β cell neighbors to modulate insulin secretion, and between heterotypic α-β cell neighbors to inhibit glucagon secretion[16,17]. Altogether, islet architecture sets up organized spatial interactions among endocrine cell types within the islet, which in turn coordinate hormone secretion to maintain normoglycemia.

Islet architecture defects and disrupted pulsatile hormone secretion are seen together in obesity, prediabetes, and diabetes[18,19]. Pulsatile insulin secretion is diminished in pre-diabetic and diabetic patients[20]. Moreover, postprandial pulsatile insulin and glucagon secretion lose their countercorrelated interdependence in prediabetes and diabetes[21,22]. Postprandial inhibition of glucagon secretion, which is highly dependent on paracrine and juxtacrine signaling among β and δ cells, is also lost[23–25]. It is possible that the islet architectural defects seen in diabetes contribute to the concomitant hormone secretion phenotypes, yet the effects of altered islet architecture itself are hard to uncouple from effects of diabetes pathology and loss of β cell maturity.

Roundabout (Robo) receptors are axon guidance molecules, whose function is required for tissue morphogenesis in many organs. We have previously shown that β cell-selective deletion of the genes for two Robo receptors, Robo1 and Robo2 (Robo βKO), during islet development in neonatal mice leads to disrupted spatial tissue organization in the islet[26].

Importantly, Robo βKO does not affect β cell differentiation or death[26]. Because the islets of Robo βKO mice are severely disorganized, yet the architectural phenotype is not linked to defects in β cell differentiation or to pathologies related to β cell damage in diabetes, they provide a useful model to test the direct effects of disrupted islet architecture on islet function and glucose homeostasis. Robo βKO islets have *in vivo* disruptions in their synchronous glucose-stimulated β cell calcium oscillations, likely due to the changes in islet architecture itself[27]. Synchronous oscillations are thought to underlie pulsatile insulin secretion, which is important for secreting correct amounts of insulin in response to glucose, for regulating glucagon and somatostatin secretion, and for robust and sensitive activation of hepatic insulin signaling.

We hypothesized that Robo βKO mice would display systemic *in vivo* defects in glucose tolerance, insulin tolerance, and balanced hormone secretion, due to changes in islet architecture that disrupt cell-cell coupling and paracrine, autocrine, and juxtacrine signaling within the islet. Here, we show that Robo βKO mice have whole-body physiological defects which manifest as reduced glucose tolerance and disrupted islet glucagon and insulin secretion.

Materials and Methods

Animals

All animal experiments were conducted in accordance with the University of Wisconsin—Madison IACUC guidelines under approved protocol number M005221. Robo βKO mice have been previously described[26,27]. Robo βKO mice were kept on a mixed background and have a constitutive deletion of Robo1 with a floxed Robo2 allele, which is deleted specifically in the β cell using either Ucn3-Cre (targeting mature β cells) or Ins1-Cre (targeting differentiated β cells). A model with a Robo1 deleted background was used in order to fully remove potential compensatory or redundant Robo signaling in the islet; however, prior work shows that Robo1 appears to be dispensable for endocrine cell type sorting and islet architecture establishment during development, with Robo2 being the primary driver of the islet architectural defect seen in Robo βKO mice[26]. All mice possessed one copy of $Rosa26^{lsl\text{-}H2B\text{-}mCherry}$ (Ref. [26]). Ucn3-Cre Robo βKO or Ins1-Cre Robo βKO mice and their respective Cre+ Robo wildtype littermate controls were enrolled when they reached at least 8 weeks of age.

Oral glucose tolerance tests

Mice were fasted starting in the morning for 6 hours by removing chow and transferring mice to a fresh cage. Glucose was administered via oral gavage at a dosage of 2g glucose/kg bodyweight. Blood glucose measurements were taken at time 0-, 15-, 30-, 60-, and 120-minutes post-gavage.

IP insulin tolerance tests

Mice were fasted starting in the morning for 6 hours by removing chow and transferring mice to a fresh cage. Insulin was administered via intraperitoneal (IP) injection at a dosage of 0.4U/kg bodyweight for males and 0.2U/kg bodyweight for females from the Ucn3-Cre

line, and 0.6U/kg bodyweight for males and 0.3U/kg bodyweight for females from the Ins1-Cre line. Dosages were optimized for each line and adjusted to account for sex differences in insulin sensitivity. Blood glucose measurements were taken at time 0-, 15-, 30-, 60-, and 120-minutes post IP injection.

In vivo measurements of glucagon during insulin tolerance test

Mice were fasted starting in the morning for 6 hours by removing chow and transferring mice to a fresh cage. Insulin was administered via intraperitoneal (IP) injection at the dosages listed above. Blood samples were collected in heparin coated tubes from the tail vein at times 0-, 15-, 30-, 60-, and 120-minutes post IP injection. Samples were kept on ice for the duration of experiment and then spun at 2000 × g for 20 minutes at 4°C to separate plasma. Plasma glucagon levels were measured using a mouse glucagon ELISA kit (CrystalChem).

In vivo measurements of insulin during glucose tolerance test

Mice were fasted starting in the morning for 6 hours by removing chow and transferring mice to a fresh cage. Glucose was administered via oral gavage at a dosage of 2g glucose/kg bodyweight. Blood samples were collected in heparin coated tubes from the tail vein at times 0-, 15-, 30-, 60-, and 120-minutes post IP injection. Samples were kept on ice for the duration of experiment and then spun at 2000 × g for 20 minutes at 4°C to separate plasma. Plasma insulin levels were then measured using an ultra-sensitive mouse insulin ELISA kit (CrystalChem).

Pancreas collection after oral gavage

Mice were fasted starting in the morning for 6 hours by removing chow and bedding. Glucose was administered via oral gavage at a dosage of 2g glucose/kg bodyweight. 5 minutes post gavage, mice were euthanized via CO_2 inhalation, and pancreata were harvested and immediately placed in 10 ml acid-ethanol (0.18M HCL in 70% EtOH)

Whole pancreas hormone content

Pancreata from Ucn3-Cre Robo βKO and wildtype controls were incubated in acid-EtOH overnight at −20°C, then homogenized and incubated overnight again at −20°C. Samples were spun at 2000 × g at 4°C for 15 minutes. Supernatant was collected and neutralized using an equal volume of Tris-HCL pH 8.0. Total protein was measured using a Bradford assay, and insulin and glucagon concentration were measured using an ultra-sensitive insulin or glucagon ELISA, respectively. Insulin and glucagon concentrations were normalized to total protein.

Measurements of lean and fat mass

Ins1-Cre Robo βKO and wildtype male and female mice were anesthetized with isofluorane and scanned using a Faxitron UltrafocusDXA (Small Animal Imaging and Radiotherapy Facility, UW Madison) to determine percentage fat and lean body mass. Results were analyzed by t-test.

Statistical analyses

Statistics were performed using GraphPad Prism. Curve differences in glucose tolerance, insulin tolerance, and insulin and glucagon secretion over time were analyzed by a repeated measures two-way ANOVA (time and genotype); interaction effect is reported unless otherwise stated. Differences in area under the curve (minus baseline) were analyzed by t-test. Differences in fasted glucose and hormone levels, whole pancreas hormone content, percent fat mass, and body weights were analyzed by t-test.

Results

Robo βKO mice have impaired glucose clearance and are hypoglycemic upon fasting

We hypothesized that disrupted islet architecture in Robo βKO mice would lead to defects in glucose tolerance due to irregular hormone secretion and reduced synchronous calcium oscillations. Thus, we first tested whether glucose tolerance defects, indicative of abnormal hormone secretion, were present in Robo βKO mice. To this end, we performed oral glucose tolerance tests (OGTT) on both male and female Robo βKO and control animals (Figure 1, **Supplemental Figure 1**). In line with our hypothesis, and concurring with our previous results using intraperitoneal glucose tolerance tests (IPGTT)[26], we observed a trend toward reduced glucose tolerance in Robo βKO male mice (ANOVA: Ucn3-Cre males p=0.0004, Ucn3-Cre females p=0.1741, Ins1-Cre males p=0.0081, Ins1-Cre females p=0.9016), with the most significant increase in area under the curve (AUC) seen in Ucn3-Cre Robo βKO males compared to wildtype controls (Ucn3-Cre males p=0.0045, Ucn3-Cre females p=0.0971, Ins1-Cre males p=0.3493, Ins1-Cre females p=0.4871). The differences in glucose excursion and increase of AUC during OGTT in Ucn3-Cre Robo βKO indicates delayed glucose clearance, suggesting defects in hormone secretion or sensing under glucose challenge. Interestingly, despite worse glucose tolerance in Robo βKO mice compared to controls, we observed a significant reduction in fasting blood glucose levels in Ucn3-Cre Robo βKO males (p=0.0477) compared to wildtype controls, while females exhibited a mild trend (p=0.2614) (Figure 1I, K). Ins1-Cre Robo βKO males, in contrast, did not show a significant difference in fasted glucose levels (p=0.7229), while Ins1-Cre Robo βKO females showed a trend toward decreased fasting glucose in comparison to wildtype controls (p=0.1286) (Figure 1J,L).

Altogether, these defects in glucose homeostasis suggest that hormone secretion in both fasted and glucose challenged states may be disrupted in Robo βKO mice, especially in males. Furthermore, the apparent discrepancy between fasted and glucose-challenged blood glucose levels indicates relative loss of glucose control overall. Thus, to further understand glucoregulation in Robo βKO mice, we next measured hormone secretion *in vivo* in response to fasting and glucose challenge.

Robo KO mice show a trend toward impaired insulin secretion in vivo

Loss of pulsatile insulin secretion is known to decrease insulin pulse mass, and thus reduce gross insulin secretion[21]. Further, loss of coordinated calcium oscillations among β cells can result in leaky insulin secretion at low glucose *in vitro*[28]. To test if Robo βKO mice have disrupted insulin secretion in response to fasting and glucose challenge, we performed *in*

vivo glucose-stimulated insulin secretion (GSIS) assays. Specifically, mice were fasted for 6 hours followed by oral glucose challenge and subsequent measurement of plasma insulin levels at timepoints during fasting and after challenge (Figure 2, **Supplemental Figure 2**). We observed a trend toward difference in insulin secretion over time after glucose challenge in most Robo βKO groups compared to controls (ANOVA: Ucn3-Cre males p=0.0566, Ucn3-Cre females p=0.3633, Ins1-Cre males p=0.0449, Ins1-Cre females p=0.1626). We also saw a reduction in AUC of insulin secretion over time in Ucn3-Cre Robo βKO (Figure 2B) male mice compared to wildtype controls, though this did not quite reach statistical significance (Ucn3-Cre Robo βKO, p=0.0658), while Ins1-Cre Robo βKO males (Figure 2D) and females of both genotypes (Figure 2F, H) appeared less affected. This suggests that the defects in pulsatile insulin secretion seen in Robo βKO mice may contribute to deficiencies in GSIS. Interestingly, despite the observation that Robo βKO males display significantly decreased fasting blood glucose levels, we observed no change in fasting plasma insulin levels in Robo βKO mice compared to controls (Figure 2I–L).

Considering this absence of hyperinsulinemia during fasting, another possible explanation for the relative fasting hypoglycemia seen in Robo βKO mice could be dysregulation of glucagon signaling. Robo βKO islets have mis-localized α cells, which would likely disrupt juxtacrine and paracrine signaling between α and β/δ cells important for regulating glucagon secretion[29–32]. Thus, to test whether glucagon secretion is perturbed in Robo βKO mice, we next measured fasted and *in vivo* insulin-stimulated glucagon secretion.

Robo βKO mice have increased fasted and insulin-stimulated glucagon secretion

Crosstalk *via* juxtacrine and paracrine signaling among α, β, and δ cells is important for regulated glucagon secretion in response to stimuli. Further, disrupted pulsatile insulin secretion is known to dysregulate glucagon secretion. Thus, to understand how these factors may affect α cell secretion in Robo βKO mice, we performed *in vivo* measurements of plasma glucagon in response to fasting and insulin challenge (Figure 3, **Supplemental Figure 3**). We found that in both Ucn3-Cre and Ins1-Cre lines, Robo βKO female mice showed significantly higher fasted plasma glucagon levels (Ucn3-Cre Robo βKO, p=0.0015; Ins1-Cre Robo βKO, p=0.0482) compared to controls, while no difference was observed in males (Figure 3A–D). Changes in plasma glucagon over time following intraperitoneal insulin challenge were significantly different in Ucn3-Cre Robo βKO females compared to wildtype controls (ANOVA, interaction effect: p=0.0006, main effect of genotype: p=0.0093), while the other groups did not exhibit a strong difference in glucagon secretion over time (ANOVA: Ucn3-Cre males p=0.6520, Ins1-Cre males p=0.8548, Ins1-Cre females p=0.4489). Similarly, AUC of plasma glucagon levels normalized to baseline were significantly higher in Ucn3-Cre Robo βKO females compared to wildtype controls (p=0.0262) (Figure 3J), while males appeared less affected (Figure 3F). In contrast, we observed a trend toward higher AUC in Ins1-Cre Robo βKO male mice compared to wildtype controls (p=0.2691) (Figure 3H), while females did not exhibit a robust difference (Figure 3L). Together with the observed decrease in insulin secretion in response to glucose challenge seen in males, this suggests that Robo βKO mice have disrupted hormone secretion consistent with defects in pulsatile insulin secretion and abnormal paracrine signaling. Thus, to see if this disrupted hormone secretion affected insulin sensitivity as

is predicted with disruptions in pulsatile secretion, we preformed insulin tolerance tests on Robo βKO mice.

Robo βKO mice have a tendency toward decreased insulin sensitivity, but show no difference in lean and fat mass

Pulsatile insulin secretion is important for keeping peripheral tissues insulin sensitive[13–15]. Thus, we predicted that if Robo βKO mice are exposed to non-pulsatile patterns of insulin secretion over their lifetime due to a decrease in synchronous calcium oscillations, they may be less insulin sensitive to exogenous insulin challenge compared to controls. To test this, we performed insulin tolerance tests on male and female Robo βKO mice and controls (Figure 4, **Supplemental Figure 4**). After a 6 hour fast, mice were injected intraperitonially (IP) with insulin, and blood glucose was measured at basal and at subsequent time points after challenge. We observed that Ucn3-Cre Robo βKO males and Ins1-Cre Robo βKO males showed a trend toward differences in glucose change over time (ANOVA: Ucn3-Cre males p=0.1339, Ins1-Cre males p=0.0540); females appeared less affected (: Ucn3-Cre females, interaction effect p=0.3469, main effect of genotype p=0.0167, Ins1-Cre females interaction effect p=0.9710, main effect of genotype p=0.0336). We found that the area over the curve of blood glucose normalized to baseline after IP insulin challenge trended toward a decrease in Ucn3-Cre Robo βKO males, though this did not reach statistical significance (p=0.1477), while females appeared unaffected (Figure 4B, F). In Ins1-Cre Robo βKO mice, neither males nor females showed a difference in ITT AUC compared to wildtype controls (Figure 4D, H). The trend seen in Robo βKO males may suggest a decrease in overall insulin sensitivity in male Robo βKO mice, yet the effect is weak if at all present.

To determine if the observed differences in glucose and insulin sensitivity and hormone secretion in Robo βKO mice was due to altered body composition, we performed analyses of lean and fat mass on Ins1-Cre Robo βKO male and female mice compared to wildtype controls using dual x-ray absorptiometry (Figure 4I–J). We saw no significant difference in ratio of lean to fat mass in either male or female Ins1-Cre Robo βKO mice compared to Ins1-Cre Robo wildtype controls, indicating that differences seen between groups are likely not attributable to differences in body composition. However, while male Ins1-Cre Robo βKO show no significant difference in body weight (Figure 4K), female Ins1-Cre Robo βKO mice weigh significantly less than their age-matched wildtype counterparts (p=0.0014) (Figure 4L).

Whole pancreas hormone content in Robo βKO mice

We observed a decrease in glucose-stimulated insulin secretion in Robo βKO males, and an increase in fasted and insulin-stimulated glucagon secretion in Robo βKO females. To test if an underlying difference in total hormone content may contribute to the different levels of hormone secretion present in Robo βKO mice, we measured whole pancreas hormone content in both sexes (Figure 5). We observed a trend toward reduced insulin (p=0.0954) and glucagon (p=0.1083) in Robo βKO males compared to controls that did not reach statistical significance. Conversely, in Robo βKO females, we found no change in insulin content and a trend toward increase in glucagon content that did not reach statistical significance (p=0.1411). Thus, it is possible that a reduction in insulin content in Robo βKO males and

an increase in glucagon content in Robo βKO females may contribute to their respective reduction in *in vivo* glucose-stimulated insulin secretion and increased fasting and *in vivo* insulin-stimulated glucagon secretion. It is possible that the small increase in glucagon seen in Ucn3-Cre Robo βKO is due in part to a higher alpha-to-β cell ratio[26].

Discussion

We show here that Robo βKO mice display systemic defects in glucose homeostasis, and glucagon and insulin secretion. Specifically, Robo βKO mice have an overall decrease in glucose tolerance and fasting glucose levels, and trend toward deficits in insulin secretion and increases in glucagon secretion compared to controls. This manifests as a trend toward decreased insulin tolerance as measured through insulin tolerance tests. There may also be differences in whole pancreas hormone content that contribute to these hormone secretion defects. Interestingly, many of these phenotypes present in a sex-specific manner that sheds further light on the relative susceptibility of different sexes to insulin and glucagon perturbations. Altogether, these physiological perturbations are in line with the hypothesis that islet architecture is important for systemic glucose homeostasis and hormone secretion *in vivo*. The small deviations from wildtype glucoregulation suggest that loss of islet architecture disrupts precision of islet function, but is not entirely required for basic islet function.

Our data support a role for islet architecture in systemic pulsatile insulin secretion. We observed a significant decrease in glucose tolerance in Robo βKO males, and a trend towards decrease in glucose tolerance in Robo βKO females. These glucose clearance defects occur concomitantly with lower plasma insulin levels in response to glucose challenge in Robo βKO males. This is in line with a defect in pulsatile insulin secretion, because non-pulsatile patterns of insulin secretion are worse at generating high plasma insulin concentration in response to glucose[21]. Together with our previous observation that Robo βKO β cells have defects in synchronous calcium oscillations which underlies insulin pulsatility[27], our data support the hypothesis that Robo βKO mice have disrupted pulsatile insulin secretion. An essential future experiment will be to measure the actual pattern of insulin secretion with higher time resolution through sampling in the portal vein of the liver[35]. This will allow for visualization of the pattern of hormone secretion over time and remove the effect of hepatic insulin clearance on circulating insulin levels.

Changes in fasting glucose, glucagon, and insulin levels and increased insulin-stimulated glucagon secretion in Robo βKO mice could suggest defects in glucose storage and utilization from the liver. Fasting hypoglycemia was observed in Robo βKO males, yet fasting insulin levels appear unchanged. Further, fasting glucagon levels are highly elevated in Robo βKO females, but this is not paired with fasting hyperglycemia. Hyper-secretion of glucagon paired with normal fasting insulin in females, and normal glucagon levels paired with fasting hypoglycemia in males, suggest defective glucose uptake and glycogen storage, or possible glycogen depletion in the liver. Additionally, we observed hyper-secretion of glucagon in response to insulin challenge in female Robo βKO mice, which could also exacerbate depletion of glycogen stores by hyperactivating liver glucose release. It is known that pulsatile insulin secretion is important for robust activation of hepatic insulin

signaling, which suppresses hepatic glucose release, and aids in glucose clearance and storage within the liver as glycogen[33]. An important future experiment will be to measure liver glycogen content to test if Robo βKO mice show a decrease in glycogen stores due to ineffective activation of hepatic insulin signaling and/or to over-secretion of glucagon and under-secretion of insulin during hyperglycemia.

Robo βKO males display a trend towards decreased insulin sensitivity to exogenous insulin compared to control males given the same dose. An important caveat is that this experiment was done by measuring endogenous insulin response to a stimulation with exogenous glucose. Thus, because overall insulin secretion in response to glucose may be lower in Robo βKO mice compared to controls (Figure 2), it could be that part of the observed reduction is due to decreased insulin secretion in general, rather than changes in the pattern of insulin secretion alone. The reduced sensitivity to exogenous insulin challenge is not due to excessive glucagon secretion in males, suggesting that an inherent insulin resistance could be present. Further experiments in which hepatic insulin signaling activation is measured after exogenous insulin challenge, where dosage can be kept consistent, may further clarify the relative contribution of insulin insensitivity and gross insulin secretion to reduced activation of hepatic insulin signaling. Additionally, euglycemic-hyperinsulinemic clamp studies would be useful in more directly measuring insulin sensitivity and insulin action in Robo βKO mice[36].

Defects in islet architecture may affect intra-islet paracrine signaling important for stimulation of pulsatile somatostatin and inhibition of glucagon secretion in response to elevated glucose. Within the islet, paracrine signaling among endocrine cells is highly coordinated. In response to pulsatile Ucn3 secretion (co-released with insulin from β cells), neighboring δ cells are stimulated to synchronously secrete somatostatin pulses that are correlated to, but slightly lag, those of insulin[7,8,12]. These somatostatin pulses in turn form a negative feedback loop with β cells to tonically inhibit insulin secretion[37,38]. Glucagon secretion in response to high glucose is also pulsatile, but exactly out of phase with insulin and somatostatin[7,8]. Pulsatile glucagon secretion is likely inhibited by the combined pulses of somatostatin and insulin and their co-secreted factors, which lower α cell cAMP levels[29], while lack of this inhibition during somatostatin/insulin pulse nadirs allows for glucagon secretion to occur[30–32]. Though counterintuitive, pulses of glucagon from α cells in response to elevated glucose are important for local stimulation of insulin secretion through the amplifying pathway *via* elevation of β cell cAMP levels[39–41]. However, it is thought that pulsatile inhibition by somatostatin stunts glucagon action enough that it does not activate hepatic glucose release, which would work counter to the action of insulin during glucose challenge[37]. This tonic control of hormone secretion by paracrine signals within the islet's microenvironment is thought to stimulate insulin secretion such that it can restore euglycemia after glucose challenge, but not to the extent that would result in hypoglycemia[37]. Thus, if intra-islet pulsatile insulin secretion is disrupted in Robo βKO mice, this would likely disrupt pulsatile somatostatin secretion and inhibition of glucagon secretion in response to high glucose. An important future experiment will be to measure plasma glucagon levels in response to a mixed meal challenge in Robo βKO mice to test for postprandial increase of glucagon secretion to a level that may affect peripheral tissues like the liver. Moreover, it would be of interest to measure intra-islet somatostatin and

glucagon secretion in response to high glucose *via* perfused pancreas experiments to capture changes that are not measurable in circulating plasma. These experiments will be necessary to better understand defects in intra-islet paracrine signaling conveyed by disruptions in islet architecture that may contribute to the disrupted hormone secretion we observe in Robo βKO mice.

An important caveat to this study is the possible contributions from Robo deletion in non-islet tissues to whole-body circulating hormone levels and glucose homeostasis phenotypes. This may explain the nuanced differences observed between the Ins1-Cre mice and the Ucn3-Cre mice In contrast to Insulin-Cre, Ucn3 is also expressed in the nervous system. Importantly, inputs from nerves have been shown to affect hormone secretion from the islets[42,43]. Since Robo has known roles in nerve development, it is possible that Ucn3-expressing nerves may have abnormal development, which could alter hormone secretion regardless of islet architectural phenotypes[44,45]. This would have been interesting to test *ex vivo*; however, this is not possible due to the tendency of Robo βKO islets to spontaneously disassociate when isolated[26]. Nevertheless, the hypersecretion of glucagon in both lines suggests that this phenotype is specific to the Robo βKO model.

Many of the physiological phenotypes we have observed in Robo βKO mice have a sex-specific manifestation. Specifically, male Robo βKO mice have decreased glucose-stimulated insulin secretion, glucose clearance defects, and increased insulin insensitivity, while female mice instead display a hyper-secretion of glucagon in both fasting and insulin challenged states, with more mild effects on fasting and glucose- or insulin-challenged plasma glucose levels. Interestingly, it has been previously reported that female mice are less sensitive to glucagon in general[46]. In contrast, male mice and humans are generally less insulin sensitive than females[47]. Thus, as insulin phenotypes are more pronounced in males due to lower insulin sensitivity and tendency towards β cell dysfunction[47], it may be that glucagon phenotypes are more exacerbated in females for similar reasons.

Acknowledgements

This work was funded in part by the following grants. R01DK121706 from the NIDDK to BB. MTA was funded by NIH Predoctoral Training Grant in Genetics 5T32GM007133-44, and a graduate training award from the UW-Madison Stem Cell and Regenerative Medicine Center. BJW was funded by a UW-Madison Endocrinology-Reproductive Physiology Training Grant number T32 HD041921.

Data Availability Statement

All data and reagents in this manuscript are available from the Authors upon reasonable request.

References

1. Kim A et al. Islet architecture: A comparative study. Islets 1, 129–136, doi:10.4161/isl.1.2.9480 (2009). [PubMed: 20606719]
2. Bonner-Weir S, Sullivan BA & Weir GC Human Islet Morphology Revisited: Human and Rodent Islets Are Not So Different After All. The journal of histochemistry and cytochemistry : official journal of the Histochemistry Society 63, 604–612, doi:10.1369/0022155415570969 (2015). [PubMed: 25604813]

3. Cabrera O et al. The unique cytoarchitecture of human pancreatic islets has implications for islet cell function. Proceedings of the National Academy of Sciences of the United States of America 103, 2334–2339, doi:10.1073/pnas.0510790103 (2006). [PubMed: 16461897]
4. Dybala MP & Hara M Heterogeneity of the Human Pancreatic Islet. Diabetes 68, 1230–1239, doi:10.2337/db19-0072 (2019). [PubMed: 30936150]
5. Hoang DT et al. A conserved rule for pancreatic islet organization. PloS one 9, e110384, doi:10.1371/journal.pone.0110384 (2014). [PubMed: 25350558]
6. Striegel DA, Hara M & Periwal V Adaptation of pancreatic islet cyto-architecture during development. Phys Biol 13, 025004, doi:10.1088/1478-3975/13/2/025004 (2016). [PubMed: 27063927]
7. Hellman B, Salehi A, Grapengiesser E & Gylfe E Isolated mouse islets respond to glucose with an initial peak of glucagon release followed by pulses of insulin and somatostatin in antisynchrony with glucagon. Biochemical and biophysical research communications 417, 1219–1223, doi:10.1016/j.bbrc.2011.12.113 (2012). [PubMed: 22227186]
8. Salehi A, Qader SS, Grapengiesser E & Hellman B Pulses of somatostatin release are slightly delayed compared with insulin and antisynchronous to glucagon. Regul Pept 144, 43–49, doi:10.1016/j.regpep.2007.06.003 (2007). [PubMed: 17628719]
9. Benninger RK, Zhang M, Head WS, Satin LS & Piston DW Gap junction coupling and calcium waves in the pancreatic islet. Biophysical journal 95, 5048–5061, doi:10.1529/biophysj.108.140863 (2008). [PubMed: 18805925]
10. Farnsworth NL, Hemmati A, Pozzoli M & Benninger RK Fluorescence recovery after photobleaching reveals regulation and distribution of connexin36 gap junction coupling within mouse islets of Langerhans. The Journal of physiology 592, 4431–4446, doi:10.1113/jphysiol.2014.276733 (2014). [PubMed: 25172942]
11. Halban PA et al. The possible importance of contact between pancreatic islet cells for the control of insulin release. Endocrinology 111, 86–94, doi:10.1210/endo-111-1-86 (1982). [PubMed: 6123433]
12. van der Meulen T et al. Urocortin3 mediates somatostatin-dependent negative feedback control of insulin secretion. Nature medicine 21, 769–776, doi:10.1038/nm.3872 (2015).
13. Matveyenko AV et al. Pulsatile portal vein insulin delivery enhances hepatic insulin action and signaling. Diabetes 61, 2269–2279, doi:10.2337/db11-1462 (2012). [PubMed: 22688333]
14. Pedersen MG & Sherman A Newcomer insulin secretory granules as a highly calcium-sensitive pool. Proceedings of the National Academy of Sciences of the United States of America 106, 7432–7436, doi:10.1073/pnas.0901202106 (2009). [PubMed: 19372374]
15. Satin LS, Butler PC, Ha J & Sherman AS Pulsatile insulin secretion, impaired glucose tolerance and type 2 diabetes. Mol Aspects Med 42, 61–77, doi:10.1016/j.mam.2015.01.003 (2015). [PubMed: 25637831]
16. Konstantinova I et al. EphA-Ephrin-A-mediated beta cell communication regulates insulin secretion from pancreatic islets. Cell 129, 359–370, doi:10.1016/j.cell.2007.02.044 (2007). [PubMed: 17448994]
17. Hutchens T & Piston DW EphA4 Receptor Forward Signaling Inhibits Glucagon Secretion From alpha-Cells. Diabetes 64, 3839–3851, doi:10.2337/db15-0488 (2015). [PubMed: 26251403]
18. Kilimnik G et al. Altered islet composition and disproportionate loss of large islets in patients with type 2 diabetes. PloS one 6, e27445, doi:10.1371/journal.pone.0027445 (2011). [PubMed: 22102895]
19. Starich GH, Zafirova M, Jablenska R, Petkov P & Lardinois CK A morphological and immunohistochemical investigation of endocrine pancreata from obese ob+/ob+ mice. Acta histochemica 90, 93–101, doi:10.1016/S0065-1281(11)80167-4 (1991). [PubMed: 1675542]
20. Lang DA, Matthews DR, Burnett M & Turner RC Brief, irregular oscillations of basal plasma insulin and glucose concentrations in diabetic man. Diabetes 30, 435–439, doi:10.2337/diab.30.5.435 (1981). [PubMed: 7014311]
21. Menge BA et al. Loss of inverse relationship between pulsatile insulin and glucagon secretion in patients with type 2 diabetes. Diabetes 60, 2160–2168, doi:10.2337/db11-0251 (2011). [PubMed: 21677283]

22. Meier JJ, Kjems LL, Veldhuis JD, Lefebvre P & Butler PC Postprandial suppression of glucagon secretion depends on intact pulsatile insulin secretion: further evidence for the intraislet insulin hypothesis. Diabetes 55, 1051–1056, doi:10.2337/diabetes.55.04.06.db05-1449 (2006). [PubMed: 16567528]

23. Dinneen S, Alzaid A, Turk D & Rizza R Failure of glucagon suppression contributes to postprandial hyperglycaemia in IDDM. Diabetologia 38, 337–343, doi:10.1007/BF00400639 (1995). [PubMed: 7758881]

24. Omar-Hmeadi M, Lund PE, Gandasi NR, Tengholm A & Barg S Paracrine control of alpha-cell glucagon exocytosis is compromised in human type-2 diabetes. Nature communications 11, 1896, doi:10.1038/s41467-020-15717-8 (2020).

25. Shah P et al. Lack of suppression of glucagon contributes to postprandial hyperglycemia in subjects with type 2 diabetes mellitus. The Journal of clinical endocrinology and metabolism 85, 4053–4059, doi:10.1210/jcem.85.11.6993 (2000). [PubMed: 11095432]

26. Adams MT, Gilbert JM, Hinojosa Paiz J, Bowman FM & Blum B Endocrine cell type sorting and mature architecture in the islets of Langerhans require expression of Roundabout receptors in beta cells. Scientific reports 8, 10876, doi:10.1038/s41598-018-29118-x (2018). [PubMed: 30022126]

27. Adams MT et al. Reduced synchroneity of intra-islet Ca(2+) oscillations in vivo in Robo-deficient beta cells. eLife 10, doi:10.7554/eLife.61308 (2021).

28. Ravier MA et al. Loss of connexin36 channels alters beta-cell coupling, islet synchronization of glucose-induced Ca2+ and insulin oscillations, and basal insulin release. Diabetes 54, 1798–1807, doi:10.2337/diabetes.54.6.1798 (2005). [PubMed: 15919802]

29. Elliott AD, Ustione A & Piston DW Somatostatin and insulin mediate glucose-inhibited glucagon secretion in the pancreatic alpha-cell by lowering cAMP. American journal of physiology. Endocrinology and metabolism 308, E130–143, doi:10.1152/ajpendo.00344.2014 (2015). [PubMed: 25406263]

30. Gylfe E & Tengholm A Neurotransmitter control of islet hormone pulsatility. Diabetes, obesity & metabolism 16 Suppl 1, 102–110, doi:10.1111/dom.12345 (2014).

31. Huising MO Paracrine regulation of insulin secretion. Diabetologia 63, 2057–2063, doi:10.1007/s00125-020-05213-5 (2020). [PubMed: 32894316]

32. Xu SFS, Andersen DB, Izarzugaza JMG, Kuhre RE & Holst JJ In the rat pancreas, somatostatin tonically inhibits glucagon secretion and is required for glucose-induced inhibition of glucagon secretion. Acta Physiol (Oxf) 229, e13464, doi:10.1111/apha.13464 (2020). [PubMed: 32145704]

33. Petersen MC & Shulman GI Mechanisms of Insulin Action and Insulin Resistance. Physiol Rev 98, 2133–2223, doi:10.1152/physrev.00063.2017 (2018). [PubMed: 30067154]

34. Boucher J, Kleinridders A & Kahn CR Insulin receptor signaling in normal and insulin-resistant states. Cold Spring Harbor perspectives in biology 6, doi:10.1101/cshperspect.a009191 (2014).

35. Matveyenko AV, Veldhuis JD & Butler PC Measurement of pulsatile insulin secretion in the rat: direct sampling from the hepatic portal vein. American journal of physiology. Endocrinology and metabolism 295, E569–574, doi:10.1152/ajpendo.90335.2008 (2008). [PubMed: 18577690]

36. Ayala JE et al. Hyperinsulinemic-euglycemic clamps in conscious, unrestrained mice. J Vis Exp, doi:10.3791/3188 (2011).

37. Huising MO, van der Meulen T, Huang JL, Pourhosseinzadeh MS & Noguchi GM The Difference delta-Cells Make in Glucose Control. Physiology (Bethesda) 33, 403–411, doi:10.1152/physiol.00029.2018 (2018). [PubMed: 30303773]

38. Johnson DG, Ensinck JW, Koerker D, Palmer J & Goodner CJ Inhibition of glucagon and insulin secretion by somatostatin in the rat pancreas perfused in situ. Endocrinology 96, 370–374, doi:10.1210/endo-96-2-370 (1975). [PubMed: 1089535]

39. Capozzi ME et al. Glucagon lowers glycemia when beta-cells are active. JCI Insight 5, doi:10.1172/jci.insight.129954 (2019).

40. Rodriguez-Diaz R et al. Paracrine Interactions within the Pancreatic Islet Determine the Glycemic Set Point. Cell metabolism 27, 549–558 e544, doi:10.1016/j.cmet.2018.01.015 (2018). [PubMed: 29514065]

41. Svendsen B et al. Insulin Secretion Depends on Intra-islet Glucagon Signaling. Cell reports 25, 1127–1134 e1122, doi:10.1016/j.celrep.2018.10.018 (2018). [PubMed: 30380405]

42. Gylfe E, Grapengiesser E, Dansk H & Hellman B The neurotransmitter ATP triggers Ca2+ responses promoting coordination of pancreatic islet oscillations. Pancreas 41, 258–263, doi:10.1097/MPA.0b013e3182240586 (2012). [PubMed: 22076565]

43. Zhang M et al. Long lasting synchronization of calcium oscillations by cholinergic stimulation in isolated pancreatic islets. Biophysical journal 95, 4676–4688, doi:10.1529/biophysj.107.125088 (2008). [PubMed: 18708464]

44. Blockus H & Chedotal A Slit-Robo signaling. Development 143, 3037–3044, doi:10.1242/dev.132829 (2016). [PubMed: 27578174]

45. Blockus H et al. Synaptogenic activity of the axon guidance molecule Robo2 underlies hippocampal circuit function. Cell reports 37, 109828, doi:10.1016/j.celrep.2021.109828 (2021). [PubMed: 34686348]

46. Medak KD, Shamshoum H, Peppler WT & Wright DC GLP1 receptor agonism protects against acute olanzapine-induced hyperglycemia. American journal of physiology. Endocrinology and metabolism 319, E1101–E1111, doi:10.1152/ajpendo.00309.2020 (2020). [PubMed: 33017220]

47. Gannon M, Kulkarni RN, Tse HM & Mauvais-Jarvis F Sex differences underlying pancreatic islet biology and its dysfunction. Molecular metabolism 15, 82–91, doi:10.1016/j.molmet.2018.05.017 (2018). [PubMed: 29891438]

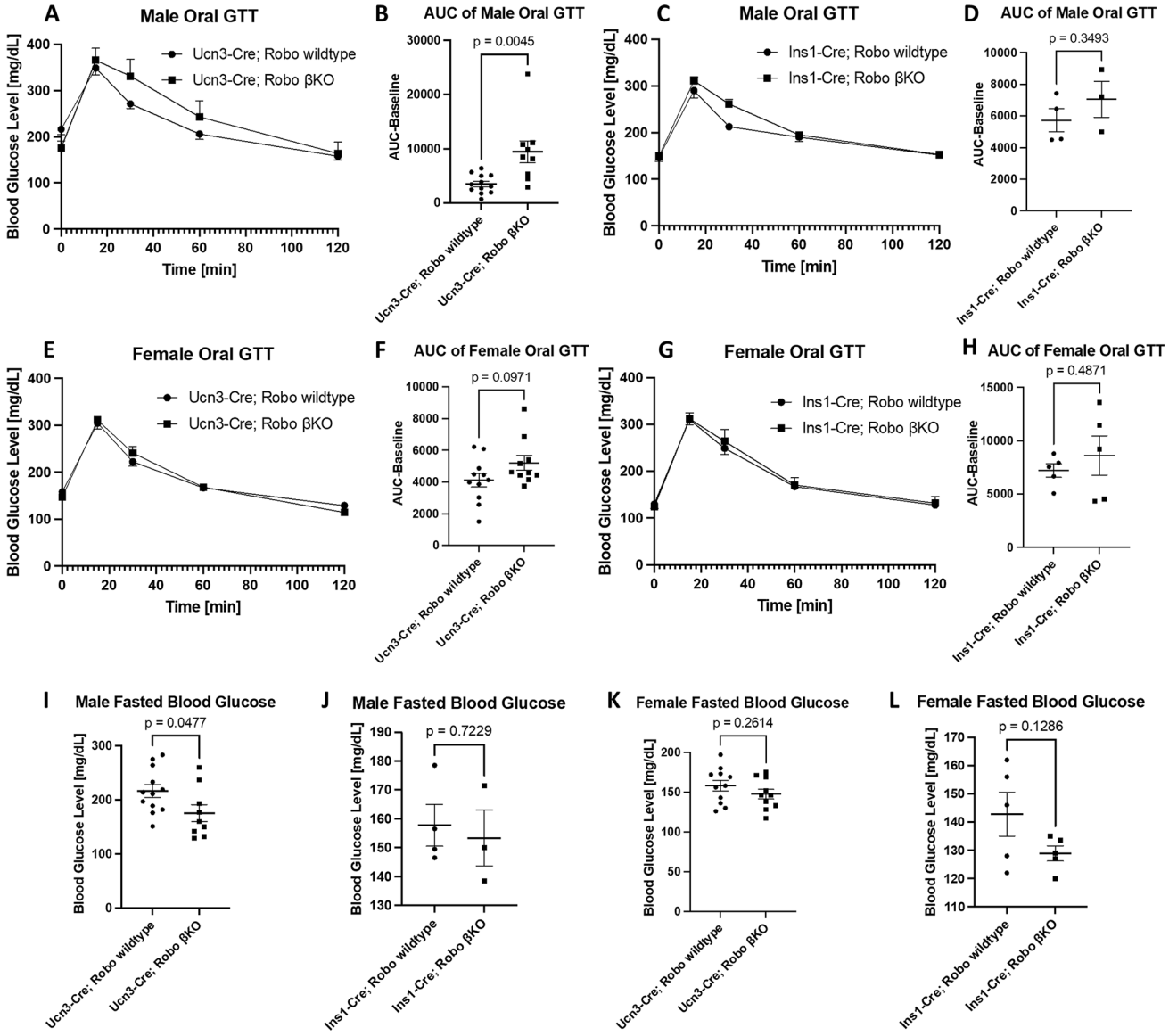

Figure 1: Plasma blood glucose levels in fasting and oral glucose challenged Robo βKO male and female mice

(**A**) Plasma glucose levels over 120 minutes after oral glucose challenge in male Ucn3-Cre Robo βKO (n=12) and Ucn3-Cre Robo wildtype (n=9) mice. (**B**) Area under the curve (AUC) of oral GTT of males shown in (A). (**C**) Plasma glucose levels over 120 minutes after oral glucose challenge in male Ins1-Cre Robo βKO (n=3) and Ins1-Cre Robo wildtype (n=4) mice. (**D**) AUC of oral GTT of males shown in (C). (**E**) Plasma glucose levels over 120 minutes after oral glucose challenge in female Ucn3-Cre Robo βKO (n=11) and Ucn3-Cre Robo wildtype (n=10) mice. (**F**) AUC of oral GTT in females shown in (E). (**G**) Plasma glucose levels over 120 minutes after oral glucose challenge in female Ins1-Cre Robo βKO (n=5) and Ins1-Cre Robo wildtype (n=5) mice. (**H**) AUC of oral GTT in females shown in (G). (**I-J**) Plasma blood glucose levels in Ucn3-Cre Robo wildtype and Robo βKO males (I) and Ins1-Cre Robo wildtype and Robo βKO males (J) after 6 hour fast. (**K-L**) Plasma blood glucose levels in Ucn3-Cre Robo wildtype and Robo βKO females (K) and Ins1-Cre

Robo wildtype and Robo βKO females (L) after 6 hour fast. Ins1-Cre fasted blood glucose measures are averages of two fasted measures.

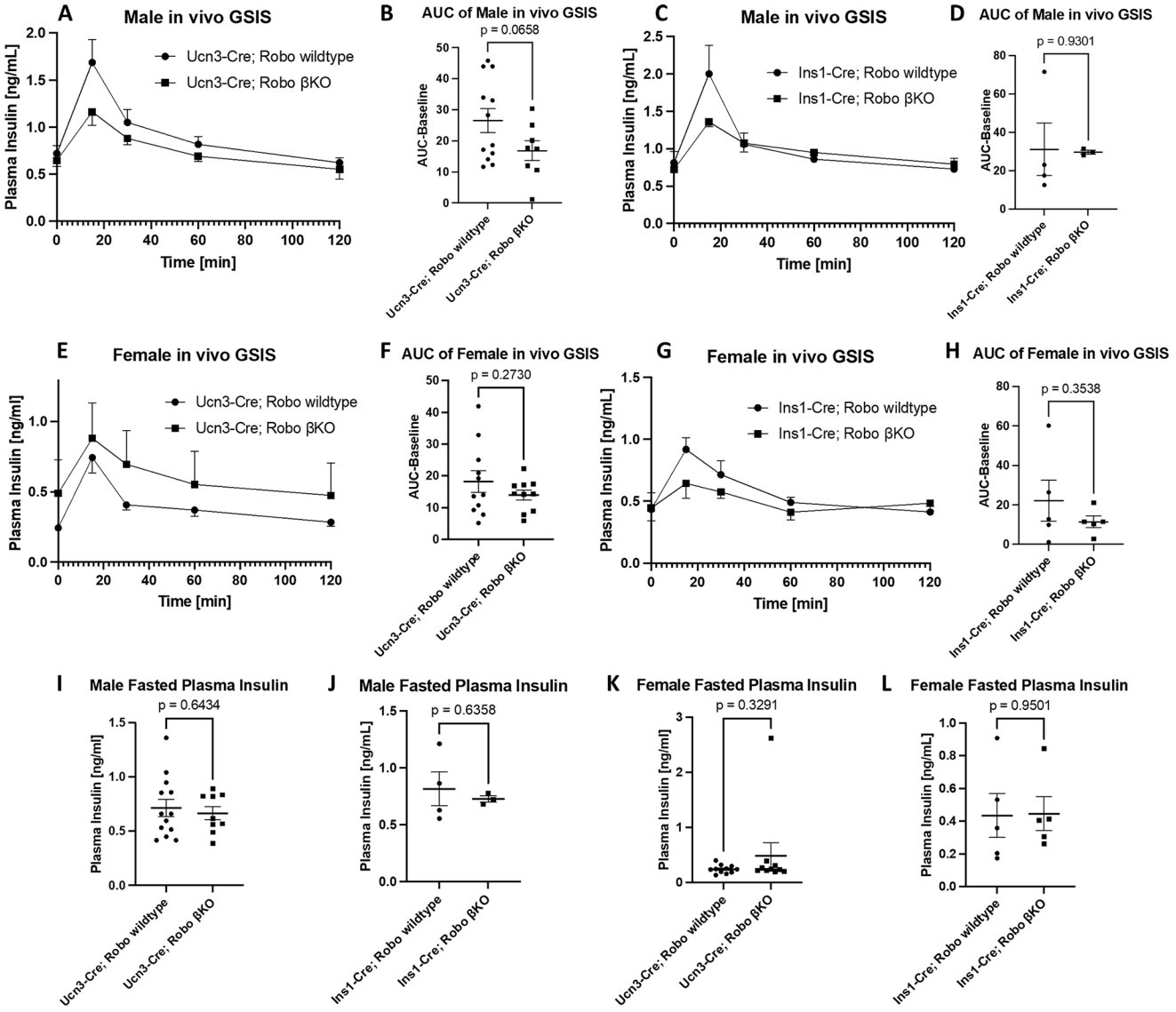

Figure 2: *in vivo* fasting and glucose-stimulated plasma insulin levels in Robo βKO male and female mice

(**A**) Plasma insulin levels over 120 minutes after oral glucose challenge in male Ucn3-Cre Robo βKO (n=12) and Ucn3-Cre Robo wildtype (n=8) mice. (**B**) Area under the curve (AUC) of in vivo GSIS in males shown in (A). (**C**) Plasma insulin levels over 120 minutes after oral glucose challenge in male Ins1-Cre Robo βKO (n=3) and Ins1-Cre Robo wildtype (n=4) mice. (**D**) Area under the curve (AUC) of in vivo GSIS in males shown in (C). (**E**) Plasma insulin levels over 120 minutes after oral glucose challenge in female Ucn3-Cre Robo βKO (n=11) and Ucn3-Cre Robo wildtype (n=10) mice. (**F**) AUC of in vivo GSIS in females shown in (E). (**G**) Plasma insulin levels over 120 minutes after oral glucose challenge in female Ins1-Cre Robo βKO (n=5) and Ins1-Cre Robo wildtype (n=5) mice showing no significant difference in insulin levels over time. (**H**) AUC of in vivo GSIS in females shown in (G). (**I-J**) Plasma insulin levels in Ucn3-Cre Robo wildtype and Robo βKO males (I) and Ins1-Cre Robo wildtype and Robo βKO males (J) after 6 hour fast. (**K-L**)

Plasma insulin levels in Ucn3-Cre Robo wildtype and Robo βKO females (K) and Ins1-Cre Robo wildtype and Robo βKO females (L) after 6 hour fast.

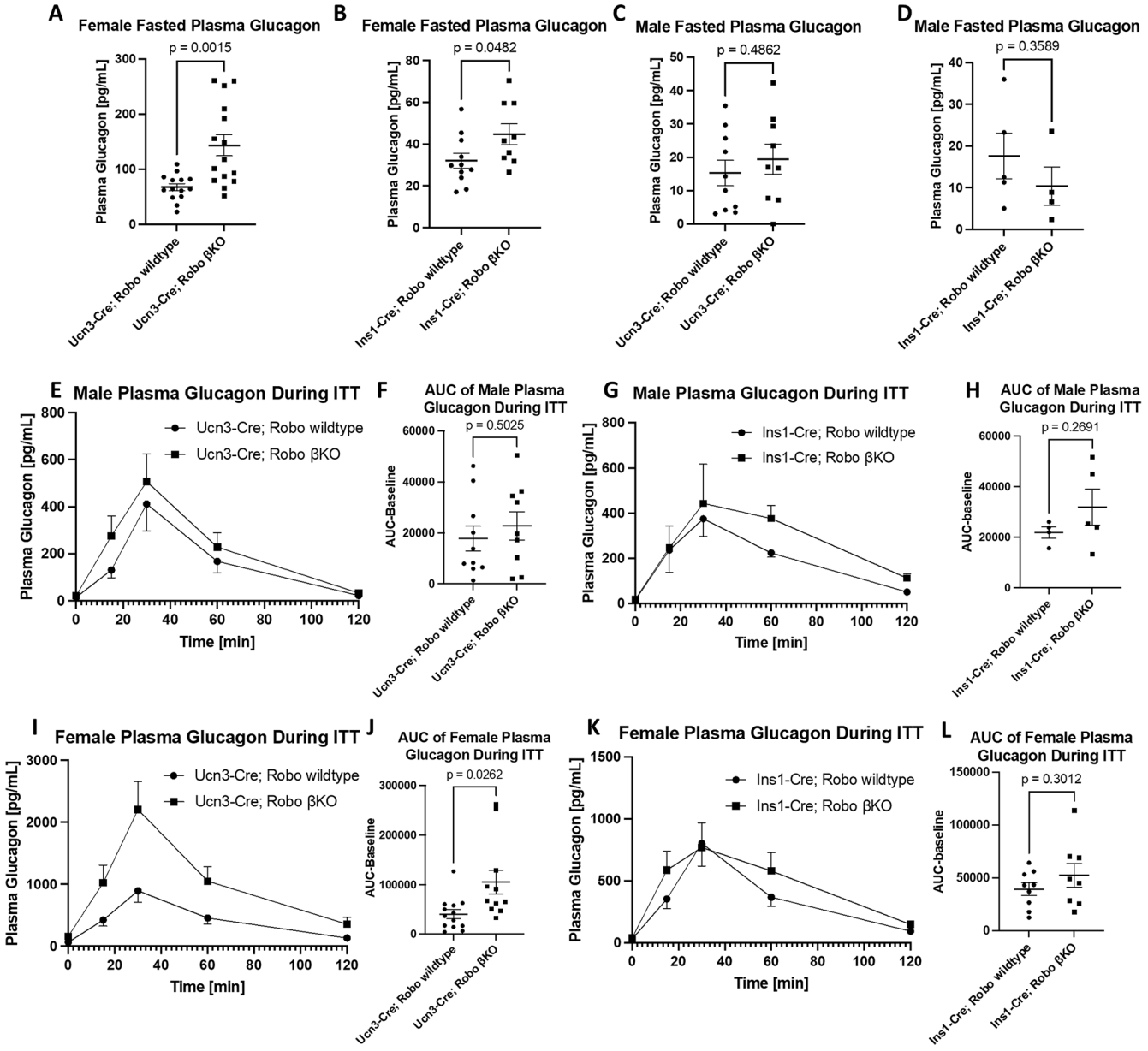

Figure 3: *in vivo* fasting and insulin-stimulated plasma glucagon levels in Robo βKO male and female mice

(**A-B**) Plasma glucagon levels in Ucn3-Cre Robo wildtype (n=14) and Robo βKO females (n=15) (A) and Ins1-Cre Robo wildtype (n=11) and Robo βKO females (n=9) (B) after 6 hour fast. (**C-D**) Plasma glucagon levels in Ucn3-Cre Robo wildtype (n=10) and Robo βKO males (n=9) (C) and Ins1-Cre Robo wildtype (n=5) and Robo βKO males (n=4) (D) after 6 hour fast. (**E**) Plasma glucagon levels over 120 minutes after IP insulin challenge in male Ucn3-Cre Robo βKO (n=10) and Ucn3-Cre Robo wildtype (n=9) mice. (**F**) Area under the curve (AUC) of in vivo insulin stimulated glucagon secretion (ISGS) in males shown in (E). (**G**) Plasma glucagon levels over 120 minutes after IP insulin challenge in male Ins1-Cre Robo βKO (n=5) and Ins1-Cre Robo wildtype (n=4) mice. (**H**) AUC of in vivo ISGS in males shown in (G). (**I**) Plasma glucagon levels over 120 minutes after IP insulin challenge

in female Ucn3-Cre Robo βKO (n=11) and Ucn3-Cre Robo wildtype (n=10) mice. (**J**) AUC of in vivo ISGS in females shown in (I). (**K**) Plasma glucagon levels over 120 minutes after IP insulin challenge in female Ins1-Cre Robo βKO (n=8) and Ins1-Cre Robo wildtype (n=9) mice. (**L**) AUC of in vivo ISGS in females shown in (K).

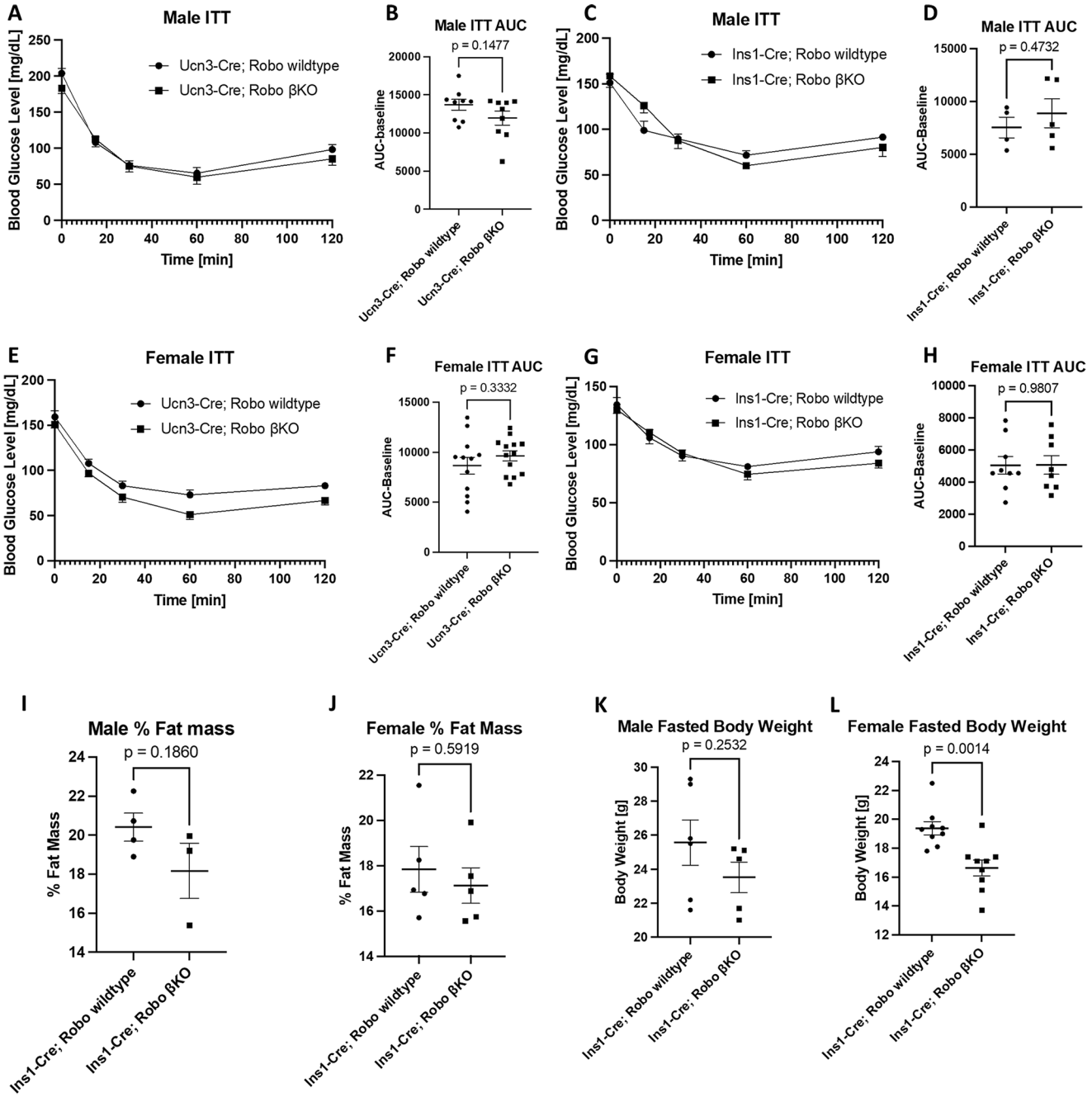

Figure 4: Insulin tolerance in Robo βKO mice, percent fat mass and total bodyweight in male and female Ins1-Cre Robo βKO mice

(**A**) Plasma glucose levels over 120 minutes after IP insulin challenge in male Ucn3-Cre Robo βKO (n=9) and Ucn3-Cre Robo wildtype (n=9) mice. (**B**) Area under the curve (AUC) of IP insulin tolerance test (ITT) in males shown in (A). (**C**) Plasma glucose levels over 120 minutes after IP insulin challenge in male Ins1-Cre Robo βKO (n=5) and Ins1-Cre Robo wildtype (n=4) mice. (**D**) Area under the curve (AUC) of IP insulin tolerance test (ITT) in males shown in (C). (**E**) Plasma glucose levels over 120 minutes after IP insulin challenge in female Ucn3-Cre Robo βKO (n=12) and Ucn3-Cre Robo wildtype (n=13) mice. (**F**) Area

under the curve (AUC) of IP ITT in females shown in (E). (**G**) Plasma glucose levels over 120 minutes after IP insulin challenge in female Ins-Cre Robo βKO (n=8) and Ins1-Cre Robo wildtype (n=9) mice. (**H**) Area under the curve (AUC) of IP ITT in females shown in (G). (**I**) Percent fat mass of male Ins1-Cre Robo βKO (n=3) and Ins1-Cre Robo wildtype (n=4) mice. (**J**) Percent fat mass of female Ins1-Cre Robo βKO (n=5) and Ins1-Cre Robo wildtype (n=5) mice. (**K**) Total fasted bodyweight of male Ins1-Cre Robo βKO (n=5) and Ins1-Cre Robo wildtype (n=6) mice. (**L**) Total fasted bodyweight of female Ins1-Cre Robo βKO (n=9) and Ins1-Cre Robo wildtype (n=9) mice.

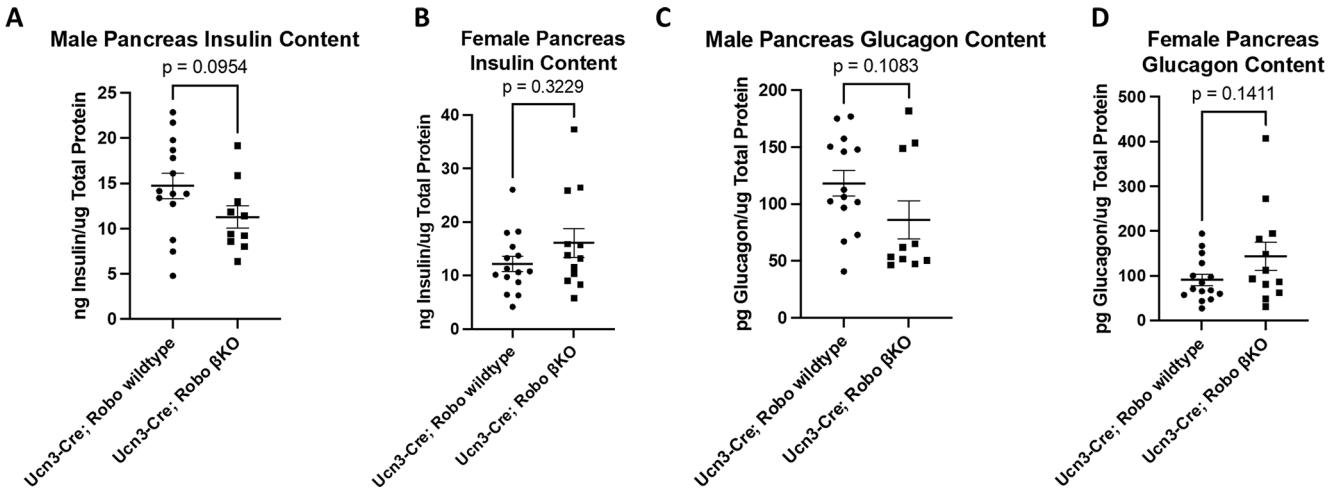

Figure 5: Whole pancreas insulin and glucagon content in Ucn3-Cre Robo βKO mice

(**A**) Whole pancreas insulin content normalized to total protein in Ucn3-Cre Robo βKO (n=14) and wildtype control (n=10) males. (**B**) Whole pancreas insulin content normalized to total protein in Ucn3-Cre Robo βKO (n=15) and wildtype control (n=12) females. (**C**) Whole pancreas glucagon content normalized to total protein in Ucn3-Cre Robo βKO (n=14) and wildtype control (n=10) males. (**D**) Whole pancreas glucagon content normalized to total protein in Ucn3-Cre Robo βKO (n=15) and wildtype control (n=12) females.